

624. Multi-degree-of-freedom modeling of mechanical snubbing systems

Sudhir Kaul

Dept. of Mechanical & Aeronautical Engineering, University of Pretoria,
Pretoria, South Africa, 0002

E-mail: *sudhir.kaul@up.ac.za*

(Received 2 January 2011; accepted 15 May 2011)

Abstract. This paper presents a multi-degree-of-freedom model for the design and analysis of mechanical snubbing in elastomeric isolators. The model consists of a three degree-of-freedom rigid body that is assembled to a rigid frame by means of elastomeric isolators and a snubbing system. The isolators are supplemented by the snubbing system so as to limit the displacement of the rigid body in all three directions of motion when the system undergoes transient loading or overloading conditions. The model is piecewise non-linear and uses normalized Bouc-Wen elements in order to capture inherent hysteresis of the elastomeric isolators and the snubbing system as well as the transition in stiffness and damping properties resulting due to inherent coupling between the isolators and the snubbing system. Separate elements are used to model the enhanced stiffness resulting from the snubbing system in the translating directions of motion. A set of elastomeric isolators and snubbing systems is used for data collection, characterization and model validation. The data collection is carried out at multiple strain amplitudes and strain rates. A conventional least squares based parameter identification technique is used for characterization. The completely characterized model is then used for simulating the response of the rigid body and the simulation results are compared to experimental data. The simulation results are found to be in general agreement with the experimental data.

Keywords: snubbing, elastomeric Isolators, Bouc-Wen, hysteresis.

1. INTRODUCTION

Mechanical snubbers are used in multiple engineering applications as displacement limiting or energy absorption devices. Mechanical snubbers are usually designed in conjunction with an isolation system in order to limit the displacement envelope of the isolated system under transient loading, or when the isolated system needs to withstand overloading conditions. Elastomeric isolators are widely used in automotive and railroad applications as passive isolation devices with the elastomer section generally designed to be in shear or compression. A commonly used snubbing system in automotive applications consists of elastomeric elements that are compressed under transient loading conditions so as to progressively limit displacement. Elastomeric isolators exhibit non-linear stiffness and damping properties, especially over a large range of strain rates and varying input displacement amplitudes. This non-linear behavior is furthermore accentuated due to the use of a mechanical snubber as a displacement limiting device. While modeling the non-linear behavior of elastomeric isolators has received a lot of attention from researchers, there is limited literature available on modeling of mechanical snubbing and integration of snubbing models with the models for elastomeric elements. Furthermore, most of the current literature on displacement limiting mechanisms uses piecewise linear models, which may not capture the transition in stiffness and hysteresis phenomena well. This work proposes an integrated piecewise non-linear multi-degree-of-

freedom model that can be used for the design and analysis of a mechanical snubbing system in conjunction with the design of a passive elastomeric isolation system.

Non-linear behavior of elastomeric isolators has been extensively studied by researchers over the last couple of decades and different modeling techniques have been used to represent specific characteristics exhibited by elastomers. Ibrahim [1] provided an extensive up-to-date review on the development of non-linear isolators and listed a thorough bibliography of research on the modeling and design of isolators with non-linear attributes. Some approaches that have been commonly used for modeling non-linear behavior such as fractional modeling and phenomenological modeling were also discussed. Berg [2] presented a model for rubber suspension components specific to railroad applications. The model was based on superposition of elastic, frictional and viscous forces and consisted of five model parameters. This model was found to be in agreement with measured results and was concluded to represent a compromise between model complexity and model accuracy. Chandrashekhar et al. [3] compared the performance of four alternate designs of a non-linear shock isolator. Based on different performance indices, the incorporation of Coulomb damping and cubic damping were concluded to enhance isolation characteristics. Kim and Singh [4] presented a model for vibration isolators in order to capture the frequency dependence of dynamic stiffness in multiple dimensions. This model, however, did not account for non-linear behavior. Shaska et al. [5] presented experimental results in order to demonstrate non-linear behavior of isolators made from butyl rubber using excitation amplitude, excitation frequency and ambient temperature as input variables. Ni et al. [6] used the general Bouc-Wen element for modeling hysteretic behavior of isolators. A frequency domain approach was proposed for identification of model parameters. Narimani et al. [7] presented a single-degree-of-freedom model for an isolator that was piecewise linear and derived a solution for the frequency response for this model. It was concluded from the parameter study that the damping ratio is a significant variable for achieving amplitude reduction. The simulation results were found to be in agreement with experimental measurements. Nguyen et al. [8] performed a parametric study in order to examine the response of an oscillator with motion limiting stops. A piecewise linear model for a single-degree-of-freedom system was used for this study and parameters like excitation amplitude, excitation frequency and stopping gap were used to study the dynamic behavior of the restrained system. Natsiavas [9] performed a stability and bifurcation analysis for a piecewise linear oscillator. A mechanical oscillator with one degree-of-freedom was studied as an example to validate results. It was concluded that the analysis could be extended to multiple degrees-of-freedom.

Unlike elastomeric isolators, there is a lack of available literature on mechanical snubbing even though the use of snubbers spans across several engineering applications, like railroad, automotive, piping systems, etc. Onesto [10] developed mathematical models to study the general characteristics of mechanical and hydraulic snubbing systems. These models were used to develop design guidelines for systems that commonly use snubbers. Chiba and Kobayashi [11] proposed a linear snubbing model with specific application to piping systems. Vibration testing was performed to determine the validity of the proposed model.

There are some similarities between the study of mechanical snubbing and certain aspects of areas of study related to vibro-impact mechanics, impact dynamics and modeling of hysteretic behavior. Some literature from these areas of study is, therefore, applicable to the study of mechanical snubbing. Luo [12] presented an analysis of an impact oscillator with a frictional slider. The design of vibro-impact machines was concluded to be an area of application for this study with specific emphasis on stability and bifurcation analysis of motion. The Bouc-Wen model has been extensively used to model non-linear and hysteretic behavior over the last few decades. Song and Kiureghian [13] proposed modifications to the conventional Bouc-Wen model, particularly for highly asymmetric hysteresis loops. The model was correlated with data from laboratory experimentation. Peterka and Vacik [14] presented a detailed synopsis of

chaotic behavior that accompanies the periodic motion of certain mechanical systems under specific excitation conditions caused by impact. The relationship between impacting bodies was based on the use of a coefficient of restitution and the transition to chaotic behavior was established in terms of existence and boundary conditions. Shaw and Holmes [15] presented a model for a non-linear oscillator that could be used to model mechanical systems which exhibit intermittent contact. The model had one degree-of-freedom and was piecewise linear, and was used to demonstrate several bifurcations resulting from varying input conditions and system properties. A large compilation of related topics and an up-to-date bibliography in contact dynamics and vibro-impact mechanics can be found in Stronge [16], with some discussion on periodic vibro-impact behavior of single degree-of-freedom systems.

There has been a phenomenal increase in literature related to the use of the Bouc-Wen model for far ranging applications. Ikhouane and Rodellar [17] classified the Bouc-Wen models into categories based on the range of governing parameters in order to relate the parameters to physical attributes. A limited range of the governing parameters was established in order to model a bounded input-bounded output system. Ikhouane and Dyke [18] further established that the generalized Bouc-Wen model is over-parametrized and may not uniquely define the input-output behavior of the modeled system. A normalized Bouc-Wen model with a reduced number of parameters was introduced so as to provide a unique input-output relationship. The normalized Bouc-Wen element has been used in this work to characterize the complete range of the force-displacement response.

This paper integrates some of the recent work done in the modeling of non-linearity and hysteresis exhibited by elastomeric isolators by providing a model that incorporates mechanical snubbing and, therefore, provides a holistic model for an isolation system and the snubbing system over a wide range of displacement amplitudes and excitation frequencies. Since most of the mechanical systems encountered in engineering practice comprise of multi-degrees-of-freedom (MDOF), consisting of either three in-plane degrees-of-freedom (DOF) or all six-DOF that a rigid body possesses in space, this paper presents a comprehensive model for a three-DOF system which incorporates the use of a mechanical snubbing system in order to limit the displacement of the system in all three directions of motion.

2. MODELING

This section presents the MDOF model consisting of a lumped mass with three in-plane DOF – two translational and one rotational, x , y and γ respectively. A representation of the model is shown in the form of a block diagram in Fig. 1 with the lumped mass that is assumed to be rigid and is assumed to undergo small rotational displacement, allowing the use of small angle approximation in the derivation of the equations of motion (EOM). The system in Fig. 1 shows a front and a rear isolator connecting the rigid body to ground. The rigid body is additionally connected to fore-aft (along x -axis) and vertical (along y -axis) snubbers at the front end as well as the rear end. The coordinate system shown in Fig. 1 will be used throughout this paper in deriving the EOM. It may be noted that the model presented in this paper is restricted to just two isolators and two pairs of translational snubbers. However, the approach adopted in this paper will be applicable to any three-DOF rigid body regardless of the number of isolators and snubbers.

The governing EOM of the system in Fig. 1 consist of three second order differential equations that are coupled with one another and are simultaneously coupled to the four first order differential equations that in turn govern the evolution of the Bouc-Wen variables, corresponding to the four Bouc-Wen elements shown in Fig. 2. The Bouc-Wen elements are used so as to capture time-dependence by the introduction of additional state variables. One Bouc-Wen element is used for each isolator in each translating direction of motion. This allows the modeling of hysteretic behavior exhibited by elastomeric systems with an appropriate

choice of model parameters. The lumped mass shown in Fig. 2 is connected to ground through the front and rear isolators located at (x_f, y_f) and (x_r, y_r) respectively, with respect to the center of mass. The displacement of the three-DOF system is constrained by the snubbers at the front end as well as at the rear end of the mass in the fore-aft (x) and the vertical (y) directions of motion. The snubber stiffness is modeled by non-linear spring elements, with k_{2fx} , k_{3fx} , k_{2fy} and k_{3fy} representing the snubbing stiffness at the front end of the rigid body in $+x$, $-x$, $+y$ and $-y$ directions respectively. The corresponding snubbing stiffness at the rear end of the rigid body is modeled with k_{2rx} , k_{3rx} , k_{2ry} and k_{3ry} representing the stiffness in $+x$, $-x$, $+y$ and $-y$ directions respectively.

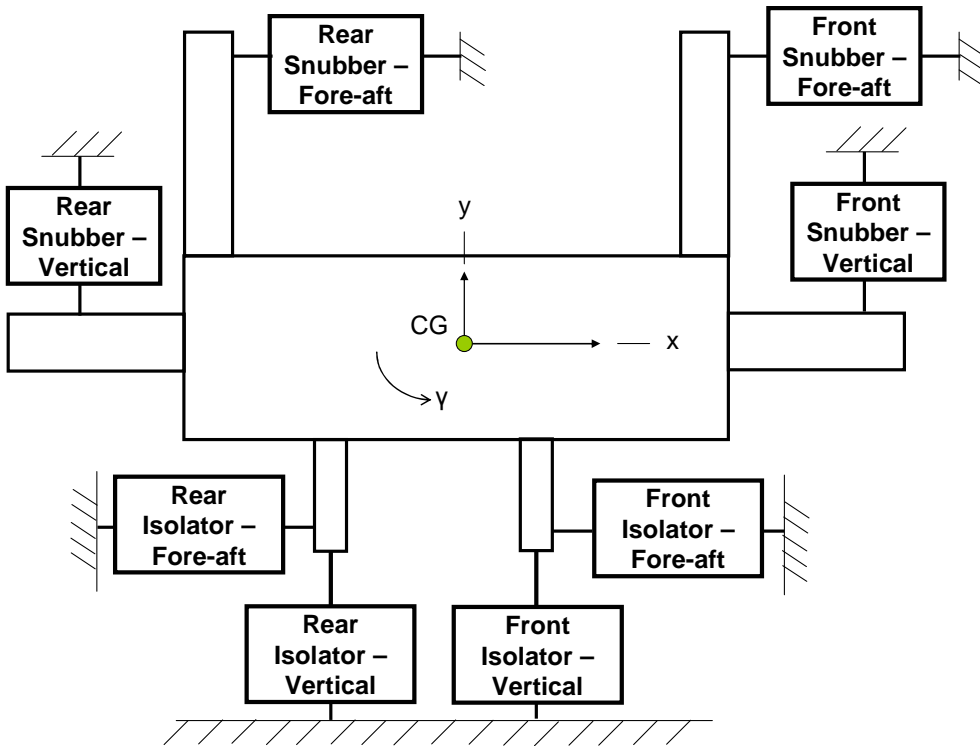


Fig. 1. Mechanical Snubbing Model – Block Diagram

The governing EOM for the fore-aft translation of the lumped mass can be expressed as follows:

$$m \ddot{x} + (b_{1fx} + b_{1rx}) \dot{x} + (k_{1fx} + k_{1rx}) x - (k_{1fx} y_f - k_{1rx} y_r) \gamma - (b_{1fx} y_f - b_{1rx} y_r) \dot{\gamma} + \alpha_{fx} w_{fx} + \alpha_{rx} w_{rx} = f_x \quad (1)$$

In Eq. (1), m is the mass of the isolated system and f_x is the excitation force acting on the mass along the x -axis at the center of mass. k_{1fx} and k_{1rx} represent the translational stiffness of the front and rear isolators along the x -axis respectively, and b_{1fx} and b_{1rx} represent the translational damping constants of the front and rear isolators along the x -axis. Eq. (1) can be alternately written as a system of two first order ordinary differential equations (ODE) as:

$$\begin{aligned} \dot{x}_1 &= x_2 \\ \dot{x}_2 &= -\frac{(k_{1fx} + k_{1rx})}{m} x_1 - \frac{(b_{1fx} + b_{1rx})}{m} x_2 + \frac{(k_{1fx} y_f - k_{1rx} y_r)}{m} x_5 \\ &+ \frac{(b_{1fx} y_f - b_{1rx} y_r)}{m} x_6 - \frac{\alpha_{fx}}{m} w_{fx} - \frac{\alpha_{rx}}{m} w_{rx} + \frac{f_x}{m} \end{aligned} \quad (2)$$

In Eqs. (1) and (2), α_{fx} and α_{rx} are the Bouc-Wen parameters that couple the system dynamics with the unit-less time-dependent variables, w_{fx} and w_{rx} , respectively as long as the two constants are non-zero. In Eq. (2), $x_1 = x$ and $x_2 = \dot{x}$. The unit-less time-dependent variables are called as the normalized Bouc-Wen variables. The damping characteristics exhibited by elastomeric isolators are primarily hysteretic. The damping constants, therefore, need to account for strain rate or excitation frequency. This is done by using the hysteresis damping constants in order to model the frequency dependence of the damping constants as:

$$b_{1pq} = \frac{h_{1pq}}{\omega} \quad (3)$$

In Eq. (3), h_{1pq} is the hysteresis damping constant, ω is the excitation frequency, the subscript 'p' can be substituted by the front and rear isolator variables 'f' and 'r' and the subscript 'q' can be substituted by the fore-aft and vertical directions 'x' and 'y' respectively to express the four damping and hysteresis constants of the model. All the damping constants from here on will be modeled as expressed in Eq. (3).

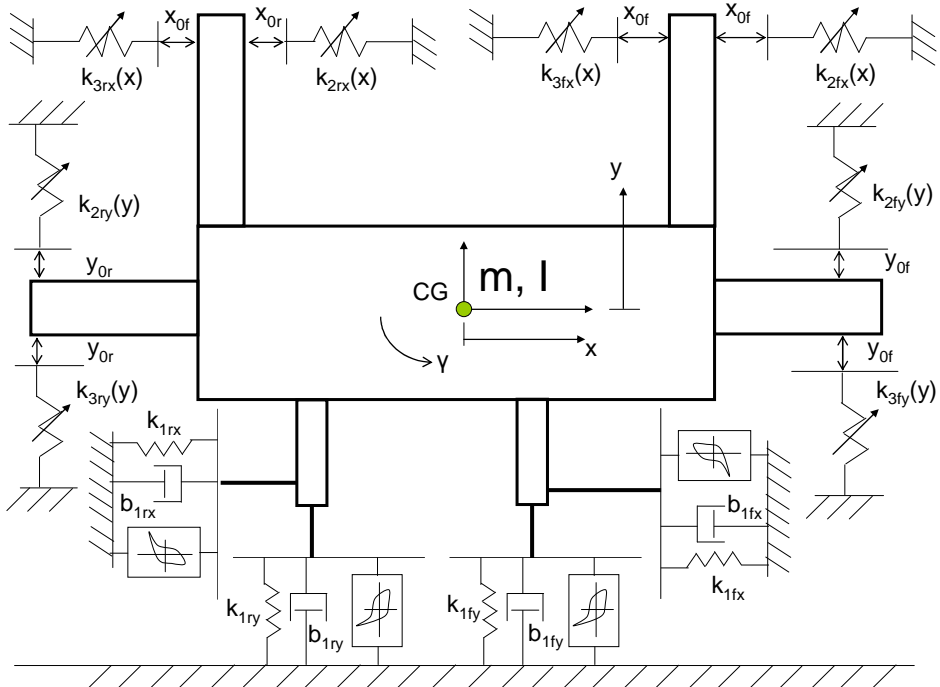


Fig. 2. Three-DOF Mechanical Snubbing Model

The governing equation for the vertical motion of the lumped mass is analogous to Eq. (1) and can be expressed as:

$$m \ddot{y} + (b_{1fy} + b_{1ry}) \dot{y} + (k_{1fy} + k_{1ry}) y + (k_{1fy} x_f - k_{1ry} x_r) \gamma + (b_{1fy} x_f - b_{1ry} x_r) \dot{\gamma} + \alpha_{fy} w_{fy} + \alpha_{ry} w_{ry} = f_y \quad (4)$$

Eq. (4) is analogous to Eq. (1) with two new Bouc-Wen parameters α_{fy} and α_{ry} coupling the system dynamics with the corresponding time-dependent variables, w_{fy} and w_{ry} , that are in turn coupled to the motion of the lumped mass in the vertical direction, along the y -axis. Eq. (4) can be alternately expressed as a system of first order equations as follows:

$$\begin{aligned} \dot{x}_3 &= x_4 \\ \dot{x}_4 &= -\frac{(k_{1fy} + k_{1ry})}{m} x_3 - \frac{(b_{1fy} + b_{1ry})}{m} x_4 - \frac{(k_{1fy} x_f - k_{1ry} x_r)}{m} x_5 \\ &\quad - \frac{(b_{1fy} x_f - b_{1ry} x_r)}{m} x_6 - \frac{\alpha_{fy}}{m} w_{fy} - \frac{\alpha_{ry}}{m} w_{ry} + \frac{f_y}{m} \end{aligned} \quad (5)$$

In Eqs. (4) and (5), f_y is the excitation force acting on the rigid body in the vertical direction, k_{1fy} and k_{1ry} represent the vertical stiffness of the front and the rear isolator respectively, and b_{1fy} and b_{1ry} represent the vertical damping constant of the front and rear isolator respectively. In Eq. (5), $x_3 = y$ and $x_4 = \dot{y}$.

The governing equation for rotational displacement of the rigid body is coupled to all four system variables incorporated in Eqs. (1) and (5), and can be expressed with the use of small angle approximation as:

$$\begin{aligned} I \ddot{\gamma} - (k_{1fx} y_f - k_{1rx} y_r) x + (k_{1fy} x_f - k_{1ry} x_r) y + (k_{1fx} y_f^2 + k_{1fy} x_f^2 + k_{1rx} y_r^2 + k_{1ry} x_r^2) \gamma \\ - (b_{1fx} y_f - b_{1rx} y_r) \dot{x} + (b_{1fy} x_f - b_{1ry} x_r) \dot{y} + (b_{1fx} y_f^2 + b_{1fy} x_f^2 + b_{1rx} y_r^2 + b_{1ry} x_r^2) \dot{\gamma} \\ - \alpha_{fx} w_{fx} y_f + \alpha_{fy} w_{fy} x_f + \alpha_{rx} w_{rx} y_r - \alpha_{ry} w_{ry} x_r = m_z \end{aligned} \quad (6)$$

In Eq. (6), m_z is the excitation moment about the z -axis acting on the mass and I is the mass moment of inertia about the z -axis at the center of mass, where the z -axis is defined as per the Right Hand rule, consistent with the coordinate system in Figs.1 and 2. Eq. (6) can be alternately written as a system of coupled differential equations as:

$$\begin{aligned} \dot{x}_5 &= x_6 \\ \dot{x}_6 &= \frac{k_{1fx} y_f - k_{1rx} y_r}{I} x_1 - \frac{k_{1fy} x_f - k_{1ry} x_r}{I} x_3 + \frac{b_{1fx} y_f - b_{1rx} y_r}{I} x_2 - \frac{b_{1fy} x_f - b_{1ry} x_r}{I} x_4 \\ &\quad - \frac{k_{1fx} y_f^2 + k_{1fy} x_f^2 + k_{1rx} y_r^2 + k_{1ry} x_r^2}{I} x_5 - \frac{b_{1fx} y_f^2 + b_{1fy} x_f^2 + b_{1rx} y_r^2 + b_{1ry} x_r^2}{I} x_6 \\ &\quad + \frac{\alpha_{fx} y_f}{I} w_{fx} - \frac{\alpha_{fy} x_f}{I} w_{fy} - \frac{\alpha_{rx} y_r}{I} w_{rx} + \frac{\alpha_{ry} x_r}{I} w_{ry} + \frac{m_z}{I} \end{aligned} \quad (7)$$

In Eq. (7), $x_5 = \gamma$ and $x_6 = \dot{\gamma}$, all the remaining variables in Eq. (7) remain identical to the variables introduced in Eqs. (1) through (6). It may be noted that the derivation of Eq. (7) is based on the assumption that the system undergoes small angular displacement. The first-order equations in Eqs. (2), (5) and (7) are the governing equations for the system only as long as the snubbing displacement thresholds at the front end and at the rear end of the system are not

exceeded, i.e. $|x - y_f \gamma| < x_{of}$, $|x + y_r \gamma| < x_{or}$, $|y + x_f \gamma| < y_{of}$ and $|y - x_r \gamma| < y_{or}$, where x_{of} and x_{or} are the fore-aft snubbing thresholds at the front and the rear end respectively, and y_{of} and y_{or} are the vertical snubbing thresholds at the front and the rear end respectively. Additionally, the system of equations is coupled to four first-order equations that govern the evolution of the time-dependent Bouc-Wen variables. The generic formulation for the Bouc-Wen variables can be expressed as follows:

$$\dot{w}_{lx} = \rho_{lx} \left[(x_2 \mp y_l x_6) - \sigma_{lx} |x_2 \mp y_l x_6| w_{lx} |w_{lx}|^{n_{lx}-1} + (\sigma_{lx} - 1)(x_2 \mp y_l x_6) |w_{lx}|^{n_{lx}} \right] \quad (8)$$

$$\dot{w}_{my} = \rho_{my} \cdot \left[(x_4 \pm x_m x_6) - \sigma_{my} |x_4 \pm x_m x_6| w_{my} |w_{my}|^{n_{my}-1} + (\sigma_{my} - 1)(x_4 \pm x_m x_6) |w_{my}|^{n_{my}} \right] \quad (9)$$

In Eqs. (8) and (9), the subscripts ‘*l*’ and ‘*m*’ can be substituted by the front and rear isolator variables ‘*f*’ and ‘*r*’ respectively to yield the four governing ODE corresponding to each Bouc-Wen variable. ρ_{ij} , σ_{ij} , and n_{ij} are the Bouc-Wen parameters associated with the characteristics of each isolator.

When the displacement at any of the snubber locations exceeds the corresponding snubbing threshold, the governing EOM must be updated to account for the snubbing stiffness. It may be noted that the effective displacement at any point on the defined mass is a combination of translation and rotation, assuming small rotations. Thus the EOM will need to be updated if any of the following conditions is satisfied:

$$\begin{aligned} x_1 - y_f x_5 &\geq x_{of} & \text{OR} & & x_1 - y_f x_5 &\leq -x_{of} \\ x_1 + y_r x_5 &\geq x_{or} & \text{OR} & & x_1 + y_r x_5 &\leq -x_{or} \\ x_3 + x_f x_5 &\geq y_{of} & \text{OR} & & x_3 + x_f x_5 &\leq -y_{of} \\ x_3 - x_r x_5 &\geq y_{or} & \text{OR} & & x_3 - x_r x_5 &\leq -y_{or} \end{aligned} \quad (10)$$

The snubber thresholds, x_{of} , x_{or} , y_{of} , y_{or} , are defined in Eq. (10) so as to be symmetrical in the fore and aft translating directions and the up and down vertical directions at each of the snubbing locations. This has been done so as to reduce the number of variables and does not limit the model in any way. This assumption can be removed without any loss of generality in the proposed model.

In order to simplify the EOM formulated in Eqs. (2), (5) and (7), the reaction forces resulting from the spring elements are used to replace the corresponding terms in the EOM by making the following substitutions:

$$\begin{aligned} f_{1fx} &= k_{1fx} (x_1 - y_f x_5) \\ f_{1rx} &= k_{1rx} (x_1 + y_r x_5) \\ f_{1fy} &= k_{1fy} (x_3 + x_f x_5) \\ f_{1ry} &= k_{1ry} (x_3 - x_r x_5) \end{aligned} \quad (11)$$

In Eq. (11), f_{1fx} and f_{1rx} are the reaction forces of the two spring elements at the front and the rear end resulting from fore-aft displacements respectively, and f_{1fy} and f_{1ry} are the reaction forces of the two spring elements at the front and rear ends resulting from vertical displacements. All the reaction forces listed in Eq. (11) hold only as long as the fore-aft and vertical displacements of the isolated mass do not exceed the snubbing thresholds. The modified

EOM of the system, expressed in Eqs. (2), (5) and (7), can be re-written using the substitutions from Eq. (11) as:

$$\begin{aligned} \dot{x}_1 &= x_2 \\ \dot{x}_2 &= -\frac{f_{1fx}}{m} - \frac{f_{1rx}}{m} - \frac{b_{1fx}}{m} (x_2 - y_f x_6) - \frac{b_{1rx}}{m} (x_2 + y_r x_6) - \frac{\alpha_{fx}}{m} w_{fx} - \frac{\alpha_{rx}}{m} w_{rx} + \frac{f_x}{m} \\ \dot{x}_3 &= x_4 \\ \dot{x}_4 &= -\frac{f_{1fy}}{m} - \frac{f_{1ry}}{m} - \frac{b_{1fy}}{m} (x_4 + x_f x_6) - \frac{b_{1ry}}{m} (x_4 - x_r x_6) - \frac{\alpha_{fy}}{m} w_{fy} - \frac{\alpha_{ry}}{m} w_{ry} + \frac{f_y}{m} \\ \dot{x}_5 &= x_6 \\ \dot{x}_6 &= f_{1fx} \frac{y_f}{I} - f_{1rx} \frac{y_r}{I} - f_{1fy} \frac{x_f}{I} + f_{1ry} \frac{x_r}{I} + \frac{b_{1fx}}{I} (x_2 - y_f x_6) y_f \\ &\quad - \frac{b_{1rx}}{I} (x_2 + y_r x_6) y_r - \frac{b_{1fy}}{I} (x_4 + x_f x_6) x_f + \frac{b_{1ry}}{I} (x_4 - x_r x_6) x_r \\ &\quad + \frac{\alpha_{fx} y_f}{I} w_{fx} - \frac{\alpha_{fy} x_f}{I} w_{fy} - \frac{\alpha_{rx} y_r}{I} w_{rx} + \frac{\alpha_{ry} x_r}{I} w_{ry} + \frac{m_z}{I} \end{aligned} \tag{12}$$

Eq. (12) is the governing EOM of the system in Fig. 1 and can be used even beyond snubbing displacement thresholds with the replacement of all the spring element reaction forces by the corresponding reaction forces resulting from the snubbing stiffness. The fore-aft displacement at the front snubber will result in the following reaction forces:

$$f_{1fx} = \begin{cases} k_{1fx} (x_1 - y_f x_5) + k_{2fx} (x_1 - y_f x_5 - x_{of}) + k_{2fx} (x_1 - y_f x_5 - x_{of})^3 \\ \text{if } x_1 - y_f x_5 \geq x_{of} \\ k_{1fx} (x_1 - y_f x_5) + k_{3fx} (x_1 - y_f x_5 + x_{of}) + k_{3fx} (x_1 - y_f x_5 + x_{of})^3 \\ \text{if } x_1 - y_f x_5 \leq -x_{of} \end{cases} \tag{13}$$

In Eq. (13), k_{2fx} is the stiffness of the spring element of the front snubber corresponding to the displacement along +x-axis whereas k_{3fx} corresponds to displacement along -x-axis at the front end. The analogous equations for the fore-aft displacement at the rear snubber can be expressed as follows:

$$f_{1rx} = \begin{cases} k_{1rx} (x_1 + y_r x_5) + k_{2rx} (x_1 + y_r x_5 - x_{or}) + k_{2rx} (x_1 + y_r x_5 - x_{or})^3 \\ \text{if } x_1 + y_r x_5 \geq x_{or} \\ k_{1rx} (x_1 + y_r x_5) + k_{3rx} (x_1 + y_r x_5 + x_{or}) + k_{3rx} (x_1 + y_r x_5 + x_{or})^3 \\ \text{if } x_1 + y_r x_5 \leq -x_{or} \end{cases} \tag{14}$$

In Eq. (14), k_{2rx} is the stiffness of the spring element of the rear snubber corresponding to the displacement along +x-axis whereas k_{3rx} corresponds to displacement along -x-axis at the rear end.

The reaction forces resulting from the spring elements in the vertical direction of motion at the front end are:

$$f_{1fy} = \begin{cases} k_{1fy} (x_3 + x_f x_5) + k_{2fy} (x_3 + x_f x_5 - y_{of}) + k_{2fy} (x_3 + x_f x_5 - y_{of})^3 \\ \text{if } x_3 + x_f x_5 \geq y_{of} \\ k_{1fy} (x_3 + x_f x_5) + k_{3fy} (x_3 + x_f x_5 + y_{of}) + k_{3fy} (x_3 + x_f x_5 + y_{of})^3 \\ \text{if } x_3 + x_f x_5 \leq -y_{of} \end{cases} \quad (15)$$

In Eq. (15), k_{2fy} is the stiffness of the spring element of the front snubber corresponding to the displacement along +y-axis whereas k_{3fy} corresponds to displacement along -y-axis at the front end.

The reaction forces resulting from the spring elements in the vertical direction of motion at the rear end of the mass are as follows:

$$f_{1ry} = \begin{cases} k_{1ry} (x_3 - x_r x_5) + k_{2ry} (x_3 - x_r x_5 - y_{or}) + k_{2ry} (x_3 - x_r x_5 - y_{or})^3 \\ \text{if } x_3 - x_r x_5 \geq y_{or} \\ k_{1ry} (x_3 - x_r x_5) + k_{3ry} (x_3 - x_r x_5 + y_{or}) + k_{3ry} (x_3 - x_r x_5 + y_{or})^3 \\ \text{if } x_3 - x_r x_5 \leq -y_{or} \end{cases} \quad (16)$$

In Eq. (16), k_{2ry} is the stiffness of the spring element of the rear snubber corresponding to the displacement along +y-axis whereas k_{3ry} corresponds to displacement along -y-axis at the rear end.

The substitution of the relevant reaction forces, from Eqs. (13) to (16), in Eq. (12) yields the updated EOM when any snubbing threshold, listed in Eq. (10), is exceeded. This provides the comprehensive model for the 3-DOF rigid body held by the front and rear isolators and additionally supplemented with mechanical snubbers for limiting displacement, as shown in Fig. 2.

The model presented in this section incorporates several parameters in addition to the stiffness and damping constants of the front and rear isolators due to incorporation of the four normalized Bouc-Wen variables. The subsequent section presents the parameter identification technique that is used to completely characterize the model presented in this section.

3. PARAMETER IDENTIFICATION

This section demonstrates the use of parameter identification in order to characterize all the constants associated with the model presented in the previous section. This paper uses a conventional least squares based identification method in order to determine all the constants associated with the front and rear isolators holding the rigid body, the constants associated with the snubbing system limiting the displacement of the rigid body and all the parameters associated with the normalized Bouc-Wen model.

The objective function used for the least squares based parameter identification is defined as follows:

$$\|f_t - f_{t,m}\| \quad (17)$$

In Eq. (17), $f_{t,m}$ is the measured time history of the force transmitted to the base frame through the isolator and the snubbing system. The measurements are made with a load cell under specific loading conditions, and will be discussed in detail in the next section. f_t is the time history of force transmitted, as predicted by the model outlined in the previous section. Eq. (17) represents the norm of the difference between the time histories and is minimized in order to compute the variables associated with the model.

The following equation expresses the force transmitted through the rear isolator and the rear snubbing system in the vertical direction as an example of the theoretical force transmitted, as predicted by the model, for the computation of the objective function in Eq. (17):

$$f_{i,ry} = \begin{cases} k_{1ry} (y - x_r \gamma) + b_{1ry} (\dot{y} - x_r \dot{\gamma}) + \alpha_{ry} w_{ry} & \text{if } |y - x_r \gamma| < y_{or} \\ k_{1ry} (y - x_r \gamma) + b_{1ry} (\dot{y} - x_r \dot{\gamma}) + \alpha_{ry} w_{ry} \\ + k_{2ry} (y - x_r \gamma - y_{or}) + k_{2ry} (y - x_r \gamma - y_{or})^3 & \text{if } y - x_r \gamma \geq y_{or} \\ k_{1ry} (y - x_r \gamma) + b_{1ry} (\dot{y} - x_r \dot{\gamma}) + \alpha_{ry} w_{ry} \\ + k_{3ry} (y - x_r \gamma + y_{or}) + k_{3ry} (y - x_r \gamma + y_{or})^3 & \text{if } y - x_r \gamma \leq -y_{or} \end{cases} \quad (18)$$

In Eq. (18), $f_{i,ry}$ is the force transmitted with k_{1ry} , k_{2ry} , k_{3ry} , b_{1ry} and α_{ry} as the parameters that need to be computed. Additionally, the Bouc-Wen variable w_{ry} is a function of the parameters σ_{ry} , ρ_{ry} and n_{ry} , which need to be computed as well. This yields a total of eight parameters associated with the characterization of the force transmitted, as expressed in Eq. (18). It may be noted that the ODE governing the Bouc-Wen variable is stiff and is solved using the ODE Toolbox in MATLAB® [19].

A similar formulation to that expressed in Eqs. (17) and (18) can be used for the rear isolator in the fore-aft direction, the front isolator in the vertical direction and the front isolator in the fore-aft direction, amounting to a total of thirty-two parameters that need to be quantified in order to completely characterize the model presented in the previous section. All the parameters introduced in the previous section can, therefore, be computed by minimizing the objective function and using appropriate bounds. The Sequential Quadratic Programming (SQP) algorithm is used for solving the optimization problem using the Optimization Toolbox in MATLAB® [19].

The introduction of the non-linear Bouc-Wen elements in the governing model can result in bifurcations. All the Bouc-Wen parameters are limited to specific bounds in order to ensure a bounded input-bounded output response [16, 17] and, therefore, avoid bifurcations resulting from the non-linear element. The governing model may also exhibit bifurcations due to the piecewise discontinuity of the proposed model. The specific parameters responsible for introducing bifurcations need to be identified and analyzed before using the model for simulation. This will be discussed further in subsequent sections. The formulation presented in this section will be used to characterize a set of isolation and snubbing systems in the subsequent section.

4. RESULTS

This section presents the outcome of parameter identification using experimental data from the characterization of a set of elastomeric isolators. The isolators are integrated with their respective snubbing systems and will be referred to as front and rear isolators from here onwards. The characterized isolators are used in the model discussed in the previous sections for simulation. The simulated response is finally compared to experimental results.

A single-axis servo hydraulic actuator is used to characterize the isolators in each of the translating directions (fore-aft and vertical). The characterization experiment is repeated four times in order to capture the characteristics of the front isolators in the fore-aft and vertical directions, and the rear isolators in the fore-aft and vertical directions. The experimental set-up for data collection is shown in Fig. 3. A fixture is designed so as to assemble the isolators, and is shown in Fig. 3 as well. The fixture is designed to be sufficiently rigid with specific adjustable features so as to accommodate both the front and rear isolator assemblies. The

experimental set-up is used to collect load-displacement data in order to characterize the front and rear isolators using the parameter identification outlined in Section 3.

Each isolator assembly is pre-loaded in order to simulate static equilibrium conditions. The isolators used for experimentation have a circular cross-section with the elastomer in shear. Each isolator assembly consists of a shaft going through the center of the elastomer section of two isolators and connected to the dynamic member of the isolators as well as the actuator. The shaft system acts as the snubbing device by progressively compressing the elastomer section after overcoming the snubbing gap. The servo-hydraulic actuator is used to provide a pre-defined displacement input at a fixed input frequency. Since the load-displacement characteristics are strain rate dependant, data is collected at several levels of excitation frequency. The input frequency is varied from 2 Hz to 12 Hz, whereas the input displacement amplitude is chosen so as to cover the entire displacement range of the isolation system. The input excitation is provided under displacement control and the reaction force, transmitted to the base frame, is measured by a load cell, as shown in Fig. 3. The reaction force is measured at a sampling frequency of 500 Hz. The data collected from some of the experimental runs is shown in Figs. 4 and 5 in the form of load-displacement curves for the front and rear isolators respectively. It may be noted that the data collection is started after a few hundred cycles of excitation to allow for the settling of the elastomer and stabilization of hysteresis. A substantial increase in stiffness and a corresponding decrease in damping can be observed in Figs. 4 and 5, which is a manifestation of snubbing beyond the displacement thresholds of + 1.5 mm and -2.5 mm for the front isolator and ± 3.25 mm for the rear isolator, in the fore-aft direction of motion. The snubbing design of the isolators tested for characterization is not symmetrical, resulting in different reaction forces in the opposite translating directions. The vertical snubbing thresholds are found to be +4.5 mm, -5.25 mm and +4.75 mm, -3.75 mm for the front and rear isolators respectively.

The data collected from the front and rear isolators is used for characterization using the least squares technique outlined in the previous section, and the results are listed in Table 1. It may be noted that all model parameters are computed repeatedly for each excitation frequency. All parameters, except the damping constant, are seen to change by less than 5% for excitation frequencies ranging from 2 to 12 Hz. As a result the arithmetic mean of these parameters can be used without a significant loss of accuracy, these values are listed in Table 1. This observation about non-linear parameters of elastomeric isolators has been made in relevant literature as well [5]. The damping constant, however, is seen to reduce with the increasing excitation frequency, and is replaced by the hysteresis damping constant as explained in Section 2. All experimentation carried out for this work is conducted at room temperature with minimal variation in environmental conditions.

The parameters listed in Table 1 for characterized front and rear isolators are used for simulating the response of a three-DOF system, as shown in Fig. 2, with a mass of 125 Kg and a mass moment of inertia of 8 Kg-m² about the center of mass. The front isolator is located at (325, 20) mm and the rear isolator is located at (-320, -55) mm with respect to the origin, defined at the center of mass. A forcing function consisting of several unit step inputs with varying amplitudes and sinusoidal inputs with frequencies ranging from 1 to 7 Hz is used as the forcing function for the three-DOF system, acting at the center of mass. The model outlined in Section 2 is used to compute the displacement history at the points on the rigid body corresponding with the location of the front and rear isolators along with the force transmitted to the frame through the front and rear isolators. It may be noted that the time domain response is computed using the following initial conditions:

$$x(0) = \dot{x}(0) = y(0) = \dot{y}(0) = \gamma(0) = \dot{\gamma}(0) = 0.$$

Also, the initial condition used for all four Bouc-Wen variables is as follows:
 $w_{fx}(0) = w_{rx}(0) = w_{fy}(0) = w_{ry}(0) = 0.$

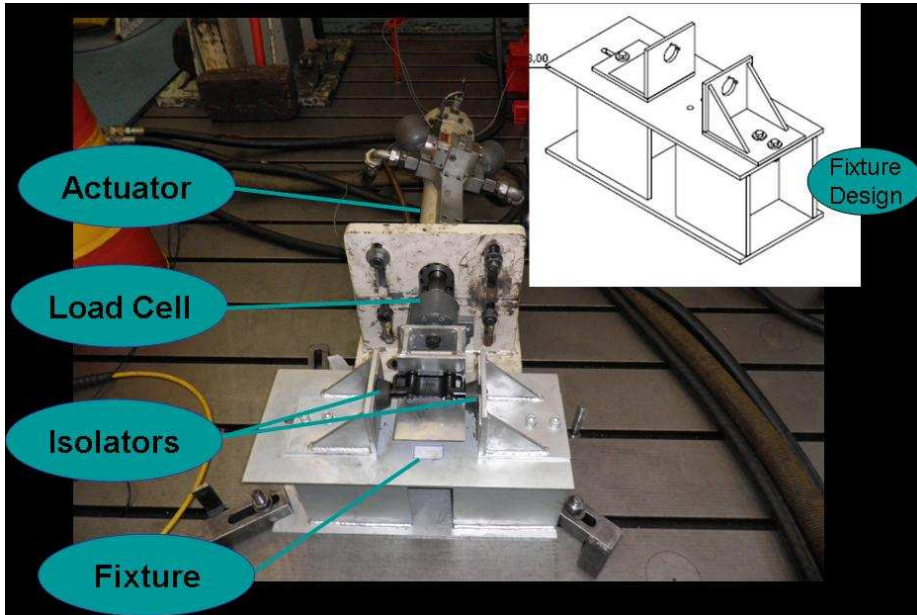


Fig. 3. Experimental Set-up

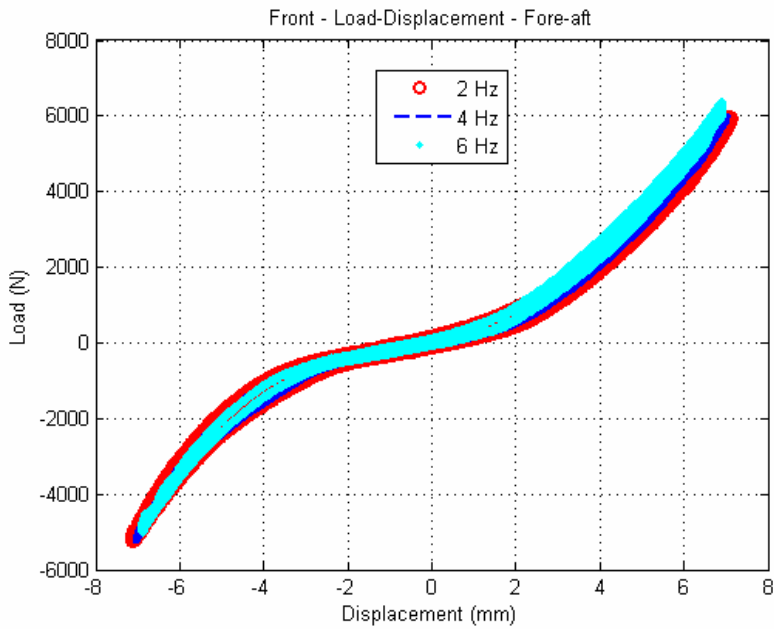


Fig. 4. Measured Force-Displacement Characteristics – Front Isolator (Fore-aft)

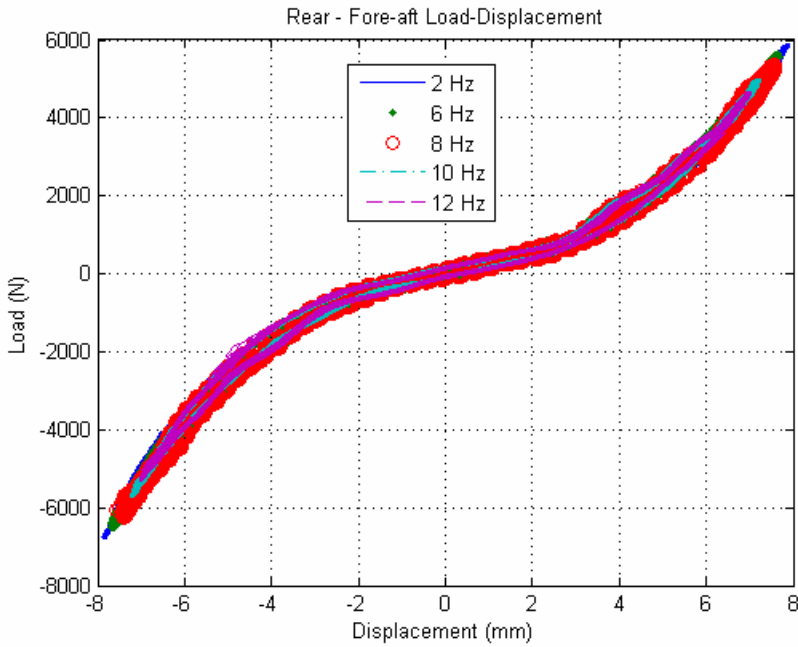


Fig. 5. Measured Force-Displacement Characteristics – Rear Isolator (Fore-aft)

Table 1. Computed Parameters

Parameters	Front Fore-aft (- fx)	Front Vertical (- fy)	Rear Fore-aft (- rx)	Rear Vertical (- ry)
k_1 (N/mm)	358.5	258.7	410.9	357.6
k_2 (N/mm)	21.7	143	29.9	83.2
k_3 (N/mm)	13.8	90.2	42.4	209.1
h_1 (N/mm)	28.4	19.5	26.9	31.3
α (N)	2.16	3.33	2.47	2.06
ρ (1/mm)	0.90	0.85	0.45	0.38
σ	0.54	0.95	0.68	1.16
n	1.70	1.54	1.31	1.69

A verification test run is performed to compare the simulation results with the measured data. The time history of displacement resulting from the simulation is used as the input to the front and rear isolators and the corresponding force transmitted to the base frame is measured, using the set up shown in Fig. 3. The simulation results are compared with the experimental data and the comparison is shown in Figs. 6 and 7. As can be seen from the two plots, the peak load between the simulated and measured response varies by less than 9% and the general load-displacement plots demonstrate similar profiles with a root mean square error of 6.17 and 7.7. All significant characteristics like the snubbing stiffness, damping and snubbing transition are successfully captured by the simulated response. These metrics serve as a validation of the proposed model. Fig. 8 shows the simulated polar plots of displacement at the front and rear isolators that can be used to comprehend the motion limiting capability of the snubbing system in order to avoid intermittent contact between the rigid body modeled in this simulation and other surrounding rigid bodies in applications with tight packaging requirements. Fig. 9 shows

the time history of all four Bouc-Wen variables for a limited interval of time. As can be seen, all four variables vary between ± 1 , satisfying the bounded input-bounded output condition for the normalized Bouc-Wen elements [18] used in the model. Furthermore, no bifurcations are exhibited by the system, which can be confirmed from the study of phase portraits. One such phase portrait, corresponding to vertical displacement at the center of mass, resulting from the simulated response is shown in Fig. 10.

5. CONCLUSIONS

A comprehensive three-DOF model has been proposed in this paper for the design and analysis of a mechanical snubbing system integrated with an elastomeric isolation system. A set of elastomeric isolators is characterized and subsequently used to demonstrate the validity of the model proposed in this paper. The model is successful in capturing the strain rate and strain amplitude dependence of the snubbing system. The model can be specifically used as an analytical tool for design iterations and design optimization in order to compute parameters like the snubbing thresholds and stiffness characteristics of the snubbing system so as to satisfy conflicting design requirements like maximizing isolation, limiting transient displacement and minimizing transmitted forces. The proposed model would also allow a designer to compute the displacement envelope around the rigid body at specific locations in order to position other components around the isolated system and avoid possible intermittent contact with these components, especially in the design of chassis assemblies in automotive applications.

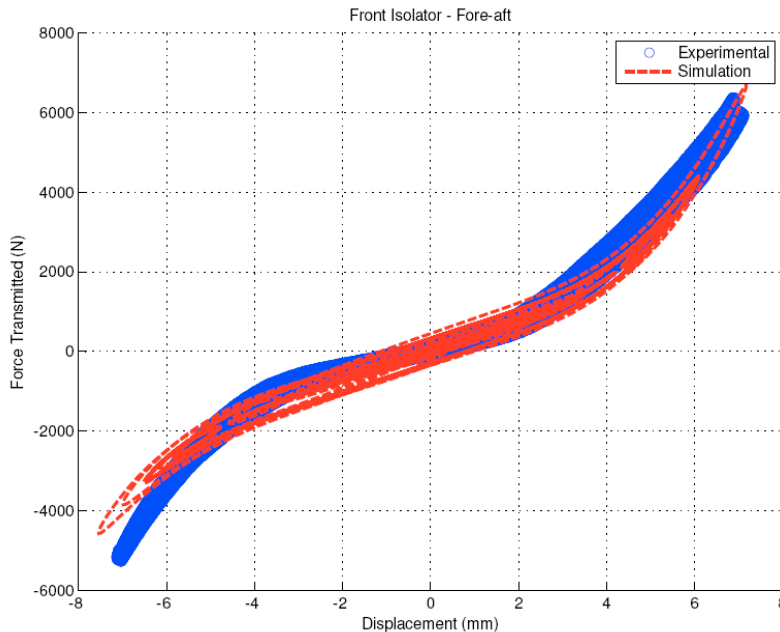


Fig. 6. Force-Displacement Characteristics – Front Isolator (Fore-aft)

Unlike other ‘motion limiting’ models in the prevailing literature for non-linear isolators and impact oscillators, the model proposed in this paper is piecewise non-linear and, therefore, is not limited to specific strain rates or displacement amplitudes over which the model can be used. Though the experimentation carried out for this work has been limited to elastomeric

isolators and snubbing systems, the formulation is generic and will be applicable to other snubbing systems or hysteretic systems as well. Non-linear isolators are known to exhibit chaotic behavior under certain excitation conditions at specific values of system parameters. Future work will focus on comprehending bifurcations with changing system parameters for the model proposed in this paper. The transition to chaotic behavior will also be studied as part of future work.

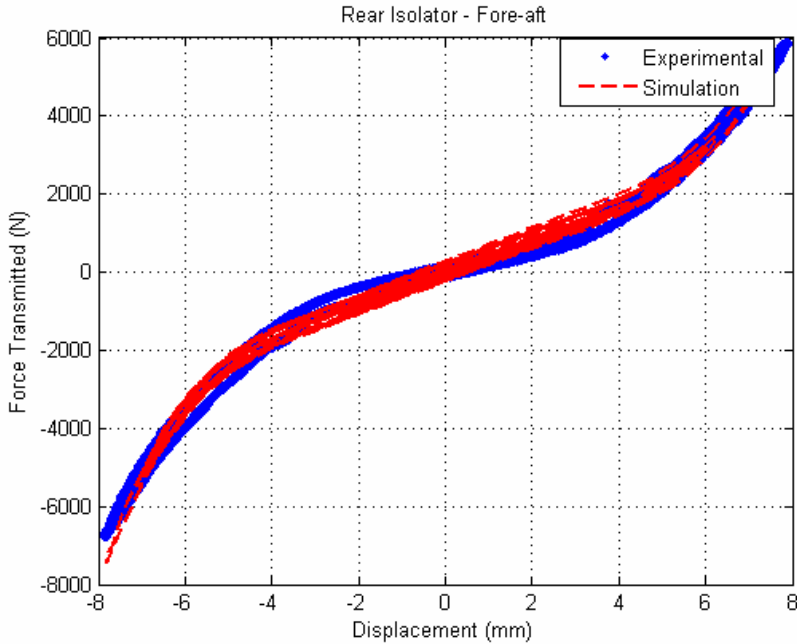


Fig. 7. Force-Displacement Characteristics – Rear Isolator (Fore-aft)

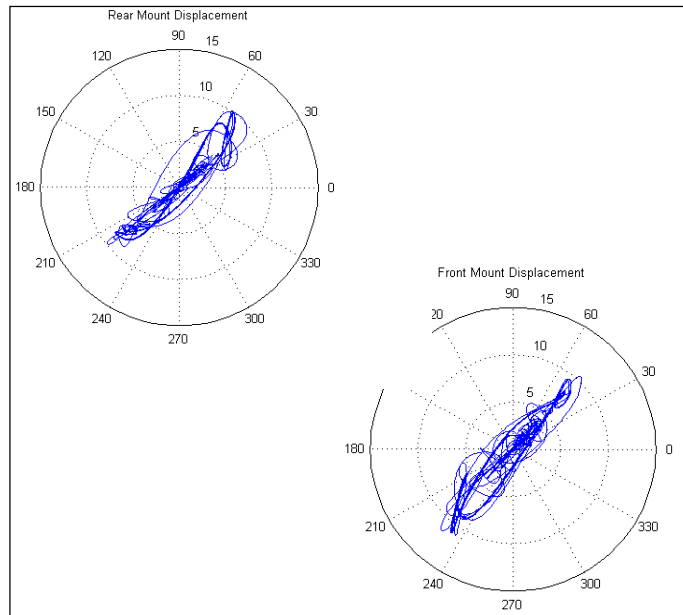


Fig. 8. Displacement Polar Plot – Rear & Front Isolators

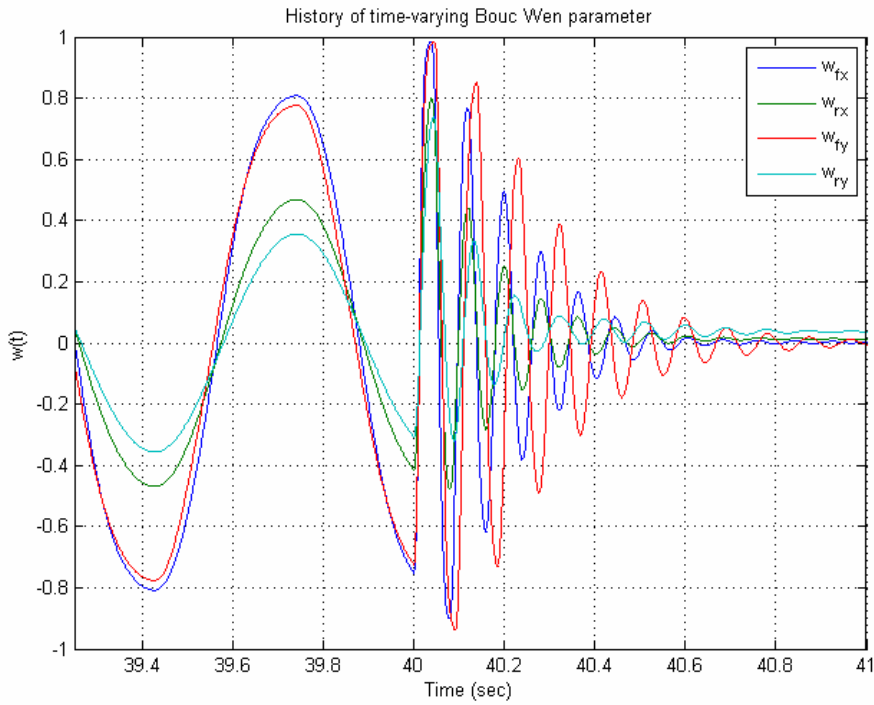


Fig. 9. Time History – Bouc-Wen Variables

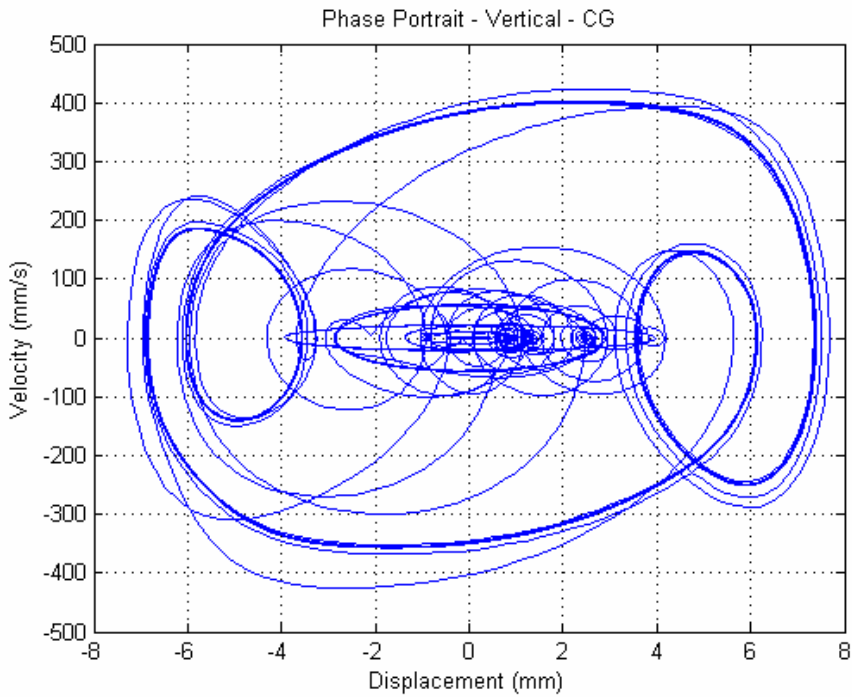


Fig. 10. Phase Portrait – Vertical Displacement

Acknowledgements

Parts for testing were provided by Product Development Center, Harley Davidson Motor Company. This support is gratefully acknowledged.

References

- [1] **Ibrahim R. A.** (2008). Recent Advances in Nonlinear Passive Vibration Isolators. *Journal of Sound and Vibration*, Vol. 314, pp. 371-452.
- [2] **Berg M.** (1998). A Non-Linear Rubber Spring Model for Rail Vehicle Dynamics Analysis. *Vehicle System Dynamics*, Vol. 30, pp. 197-212.
- [3] **Chandrashekhara N., Hatwal H., Mallik A. K.** (1999). Performance of Non-Linear Isolators and Absorbers to Shock Excitation. *Journal of Sound and Vibration*, Vol. 227, No. 2, pp. 293-307.
- [4] **Kim S., Singh R.** (2001). Multi-Dimensional Characterization of Vibration Isolators over a Wide Range of Frequencies. *Journal of Sound and Vibration*, Vol. 245, No. 5, pp. 877-913.
- [5] **Shaska K., Ibrahim R.A., Gibson R. F.** (2007). Influence of Excitation Amplitude on the Characteristics of Nonlinear Butyl Rubber Isolators. *Nonlinear Dynamics*, Vol. 47, pp. 83-104.
- [6] **Ni Y. Q., Ko J. M., Wong C. W.** (1998). Identification of Non-linear Hysteretic Isolators from Periodic Vibration Tests. *Journal of Sound and Vibration*, Vol. 217, No. 4, pp. 737-756.
- [7] **Narimani A., Golnaraghi M. F., Jazar G. N.** (2004). Frequency Response of a Piecewise Linear Vibration Isolator. *Journal of Vibration and Control*, Vol. 10, pp. 1775-1794.
- [8] **Nguyen D. T., Noah S. T., Kettleborough C. F.** (1986). Impact Behaviour of an Oscillator with Limiting Stops, Part I: A Parametric Study. *Journal of Sound and Vibration*, Vol. 109, No. 2, pp. 293-307.
- [9] **Natsiavas S.** (1998). Stability of Piecewise Linear Oscillators with Viscous and Dry Friction Damping. *Journal of Sound and Vibration*, Vol. 217, No. 3, pp. 507-522.
- [10] **Onesto A. T.** (1978). Snubber Sensitivity Study. *Energy Technology Engineering Center, ETEC-TDR-78-17*, Department of Energy, CA, USA.
- [11] **Chiba T., Kobayashi H.** (1985). A Study of Modeling the Mechanical Snubber for Dynamic Analysis. *Transactions of the International Conference on Structural Mechanics in Reactor Technology*, Vol. K, pp. 189-194, North-Holland, Amsterdam.
- [12] **Luo G., Lv X., Ma L.** (2009). Dynamics of an Impact-Progressive System. *Nonlinear Analysis: Real World Applications*, Vol. 10, pp. 665-679.
- [13] **Song J., Kiureghian A.** (2006). Generalized Bouc-Wen Model for Highly Asymmetric Hysteresis. *ASCE Journal of Engineering Mechanics*, Vol. 132, No. 6, pp. 610-618.
- [14] **Peterka F., Vacik J.** (1992). Transition to Chaotic Motion in Mechanical Systems with Impacts. *Journal of Sound and Vibration*, Vol. 154, No. 1, pp. 95-115.
- [15] **Shaw S. W., Holmes P.J.** (1983). A Periodically Forced Piecewise Linear Oscillator. *Journal of Sound and Vibration*, Vol. 90, No. 1, pp. 129-155.
- [16] **Stronge W. J.** (2000). *Impact Mechanics*, Cambridge University Press, NY, USA.
- [17] **Ikhouane F., Rodellar J.** (2007). *Systems with Hysteresis: Analysis, Identification and Control using the Bouc-Wen Model*, 1st Edition, John Wiley & Sons, NY, USA.
- [18] **Ikhouane F., Dyke S. J.** (2007). Modeling and Identification of a Shear Mode Magnetorheological Damper. *Smart Materials and Structures*, Vol. 16, pp. 605-616.
- [19] **MATLAB User Guide** (2007). MathWorks, Natick, MA, USA.